Available online at www.sciencedirect.com

ScienceDirect

Materials Today: Proceedings XX (2016) XXX–XXX

materialstoday: PROCEEDINGS

www.materialstoday.com/proceedings

PMME 2016

Performance analysis of a transparent PEM fuel cell at the optimized clamping pressure applied on its bolts

S.S.L. Rao[a], A. Shaija[a] and S. Jayaraj[a]

[a]*Department of Mechanical Engineering, National Institute of Technology Calicut, India-673601*

Abstract

Experiments were carried out on a single transparent proton exchange membrane (PEM) fuel cell with titanium gas distributor plates. Effect of the clamping pressure due to torque applied on each bolt, anode and cathode humidification temperatures, fuel cell temperature and cathode flow rate on the performance of the fuel cell are discussed in this work. Results show that the performance of fuel cell increases first to a maximum and then decreases with further increase in bolt torque. The cell performance decreases with increase in cathode humidification temperature and increases with the cell temperature. Also, humidification of anode reactant is important to improve the performance of the fuel cell. The effect of cathode flow rate is less at activation and ohmic overpotential region but it is significant at concentration overpotential region.

Keywords: Clamping pressure; Bolt torque; PEM; Polarization curve; Transparent fuel cell

1. Introduction

The interest on the performance of the proton exchange membrane (PEM) fuel cells has increased in the last few years due to their inherent advantages, such as low working temperatures, high output power density, no pollutant emissions, compact and light weight and offer superior start-up and shut down system. A single fuel cell consists of end plates, current collectors, gas distributor plates, gaskets, gas diffusion layers and proton exchange membrane, where all these components are held together by high compression, not only to prevent gas leakages but also to provide low contact resistances. Generally, an increase in compression improves the electrical conductivity, but impedes gas transport and water removal by changing the pore size distribution. The effect of compression on the fuel cell performance has been studied by several groups [1-12]. The thickness of gasket and gas diffusion layers (GDLs) and the porosity of GDL gets affected by the amount of torque exerted on the four bolts. Also, the electrical contact resistance of these layers depends on the degree to which the layers are compressed by applying torque on

Selection and Peer-review under responsibility of International Conference on Processing of Materials, Minerals and Energy (July 29th – 30th) 2016, Ongole, Andhra Pradesh, India.

its bolts. The performance and the water management in the PEM fuel cell are influenced by different operating parameters such as temperature, humidification and flow rates of the reactant gases, and GDL characteristics which are in turn dependent upon the compressive force on the membrane electrode assembly (MEA). Hence, it is essential to understand the effects of these parameters on the fuel cell operation so as to improve its performance. Among these parameters, GDL characteristics and design of the gas distributor plates are very crucial since they cannot be modified or altered during the fuel cell operation and hence have to be looked upon during the fabrication period.

Several researchers have worked on the effect of clamping pressure by applying torque on the bolts during its fabrication on the various fuel cell parameters. Lee *et al.* [1] investigated the effect of changing the bolt torque on the performance of PEM fuel cells and have obtained an optimal bolt torque. The effect of GDL compression on PEM fuel cells performance for two types of GDL materials (ELAT carbon cloth with double micro-diffusion layers and a carbon fibre paper TORAY^{TM} with an added micro-diffusion layer to the surface that was in contact with the catalyst layer) was studied experimentally by Ge *et al.* [2]. They found that the fuel cell performance, as observed through the polarization curve, first increased and then decreased with the increase in compression force after a certain value (15% of the GDL compression ratio). Zhou *et al.* [3] studied the influence of clamping force on the performance of PEM fuel cells numerically and concluded that there would be a maximum power density for an optimal clamping torque on the bolts of the fuel cell. The porosity and permeability of the GDL and electrical contact resistance between GDL and gas distributor plates was found to decrease with increase in the clamping pressure as per the experimental investigation by Chang *et al.* [4]. Ous and Arcoumanis [5] found experimentally that the performance was found to increase and then decrease with the clamping pressure in two polarization regions, ohmic and mass transport regions of the cell. The benefit of uniform pressure distribution inside a single fuel cell and fuel cell stack was demonstrated by Wang *et al.* [6] using newly designed end plates. Lin *et al.* [7] found experimentally that increasing the compression of the GDL reduced the pore volume producing high-quality contact between carbon fibres in the GDL, and between the GDL and other components. The compression ratio was found to be 60% for the optimum values of resistance, porosity and mass transfer. Wen *et al.* [8] experimentally investigated the effects of various combinations of bolt configuration and clamping torque on the corresponding contact pressure distributions and performance of a single PEM fuel cell and a 10-cells stack. A multi physics model was developed by Zhou *et al.* [9] and observed an optimum assembly pressure for the best performance of PEM fuel cell. Yim *et al.* [10] experimentally found that 5-cells PEM fuel cell showed better performance with high GDL compression for all range of currents indicating the importance of decreased contact resistance. Xing *et al.* [11] developed three-dimensional model to investigate the effect of assembly clamping pressure on the GDL properties and the performance of fuel cell. The optimization results showed that the optimum clamping pressure was different for different GDL materials. Shi *et al.* [12] numerically investigated the effect of the compressive force on the fuel cell performance focussing on the water management for various types of GDL for a variety of its parameters. The result show that both porosity and permeability of the GDL decreases after compression. The presence of liquid water also leads to an uneven distribution of the porosity and permeability. Diedrichs *et al.* [13] investigated the electrochemical performance of high temperature PEM fuel cells, membrane thickness reduction, GDL thickness loss and contact resistance between bipolar plate and GDL and between GDL and catalyst layer by compressive forces. GDL thickness loss was the main source for the observed total MEA thickness loss.

The gas distributor plates fabricated using different materials to visualize water distribution in the flow channels for various flow field patterns by different researchers are summarized in Table 1. Most of them have used stainless steel gas distributor plate since this material offers lower thickness, good mechanical stability, and clear contrast between GDL and distributor plates that is suitable for transparent PEM fuel cell. But the low chemical stability of the stainless steel makes it unsuitable for long term performance where gold plated stainless steel are used overcome this problem.

In this work, titanium plates with single serpentine flow pattern are used as gas distributor plate since it is well known for high thermal and electrical conductivities. In addition, it has high chemical stability at the operating temperatures of PEM fuel cells compared to stainless steel and it is recognized for high strength to weight ratio. The material also offers lower thickness and clear contrast between GDL and the distributor plates.

In the present study, firstly the clamping pressures resulting from torque applied on each bolt of the transparent PEM fuel cells was optimized. Later, the performance of the PEM fuel cell was studied at the optimized clamping pressure by varying the cell operating parameters such as anode and cathode humidification temperatures, cathode flow rates and the cell temperatures.

Table 1: Gas distributor plates used for transparent PEMFCs by different researchers

Gas distributor/ current collector	Flow field pattern	Active area (cm^2)	Reference
Stainless steel/Copper wire	Two straight channels	4.03	[14]
Graphite	Single channel	20.25	[15]
Gold plated stainless steel	Seven straight channels	14	[16]
-	Single serpentine and parallel channel	25	[17]
Stainless steel	Parallel, interdigitated and cascade	5	[18]
Gold plated stainless steel	Seven straight channels	14	[19]
Brass plate	Two serpentine channels	100	[20]
-	Parallel, serpentine and interdigitated	25, 100	[21]
Gold plated stainless steel	Parallel	5	[22]
Stainless steel 316	Single serpentine	10	[23]
Graphite	Serpentine	25	[24]
Graphite/gold plate	Single serpentine	25	[25]
Titanium plate	Single serpentine	25	Present investigation

2. Experimental Work

2.1 Fabrication of the transparent PEM fuel cell

The transparent PEM fuel cell fabricated in this work consist of membrane electrode assembly (MEA), gaskets, flow field plates, transparent cover plates and end plates as shown in Figure1. The MEA is composed of Nafion N212 membrane sandwiched between carbon fiber cloths which posses mechanical resilience, low density and high permeability. Platinum catalyst is considerably less active for the oxygen reduction reaction than for the hydrogen oxidation reaction, implying significant higher platinum loading in cathode as compared to the anode. Therefore, the anode and cathode are loaded with platinum of intensity 0.25 mg/cm^2 and 0.5 mg/cm^2, respectively. The MEA of 25 cm^2 is placed between the two gas distributor plates made of titanium, which is highly electrically conducting, and chemically stable which also serves as a current collector. The flow channels of both anode and cathode plates of the gas distributor plate are machined in single serpentine shape with a channel width of 2 mm, depth of 1 mm and rib width of 2 mm, as shown in Figure 2. Heater coils are then attached on the extension area of the titanium plates on both sides to increase the cell temperature. This extension area also acts like fin to reduce the cell temperature by free or forced convection when its temperature exceeded the set value. A copper block is fixed on one side of the extension area to control the operating temperature of the fuel cell. Silicone rubber sheets of 0.3 mm thickness are used on both sides of the MEA to provide the right compression force, prevent any fluid leak from the MEA and for the electrical insulation between both the anode and cathode gas distributor plates. Transparent acrylic sheets of 5 mm thickness are used on both sides of the gas distributor plates to visualize the water distribution flow behavior in the flow channel. A thick end plate made of stainless steel with a window cut out is employed on both sides to compress the transparent fuel cell and to avoid any bending effect on titanium gas distributor plates. The transparent PEM fuel cell was then clamped with four screw joints that are tightened with uniform torque.

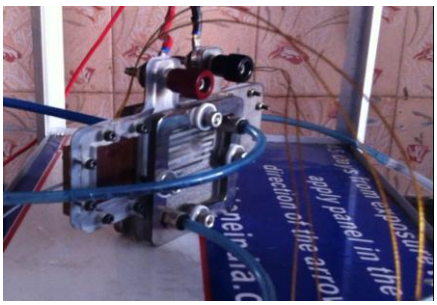

Fig. 1 Transparent single PEM fuel cell

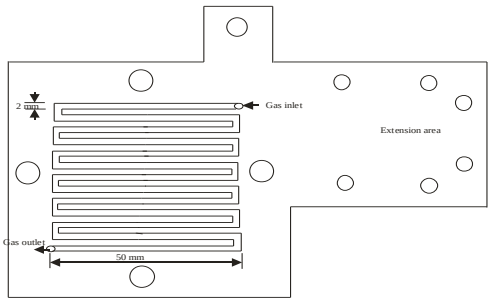

Fig.2 Schematic of titanium gas distributor plate

2.2 Experimental set-up

The transparent PEM fuel cell was tested in a fuel cell test station, the set-up fabricated and assembled by *Ingsman Energy and Fuel cell Research Organization Private Limited* (IEFRO), India as shown in Figure 3. It consisted of hydrogen and oxygen cylinders with pressure regulators, mass flow controllers for hydrogen

and oxygen, humidifiers with temperature controllers for hydrogen and oxygen, electronic load and transparent PEM fuel cell with temperature controller. High purity hydrogen (99.999%) from the metal hydride cylinder and oxygen from the cylinder were used for the experiments. The hydrogen and oxygen flow rates were regulated using mass flow controllers of AALBORG make (0-600 ml/min for hydrogen and 0-1000 ml/min for oxygen). An electronic load (10 V and 300 amps) was connected to the transparent PEM fuel cell. Temperature controllers were used to control the reactant humidification temperature and the fuel cell temperature.

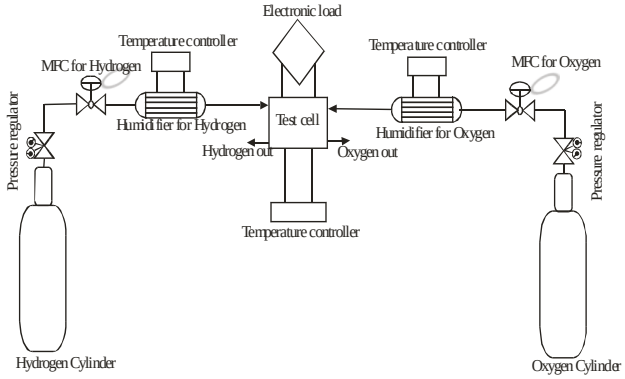

Fig.3 Schematic of Experimental set-up

3. Results and discussion

The optimum clamping pressure resulting from the torque applied on the bolts was different for different GDL materials since its electro-physical properties such as porosity, gas permeability, and contact resistance between GDL and the current collector depends on the clamping pressure [4, 11, 12]. Therefore, the first objective of this study was to optimize the clamping pressure or torque applied on each bolts to get the maximum performance of the fuel cell. Secondly, the effects of operating parameters such as, anode and cathode humidification temperatures, fuel cell operating temperature, and oxygen flow rate on the performance of the fuel cell at the optimum torque was studied.

3.1. Effect of bolt torque

Experiments were carried out to know the effect of the clamping pressures on the performance of the fuel cell by applying torque varying from 2 N.m to 3.5 N.m with an increment of 0.5 N.m on each bolt. Anode (AHT) and cathode humidification temperatures (CHT) were kept at 50°C and the fuel cell temperature (TFC) at 40°C. The flow rates were set according to the measured current at either a high or a low stoichiometry. The high stoichiometry corresponds to flow rates that were 2.0 times greater than that required by the measured current. i.e., for hydrogen 100% excess hydrogen and for air 3.5 times greater than that required for air [1]. Therefore, the hydrogen (H_2) and oxygen mass flow rates (O_2) were regulated at 100 ml/min and 200 ml/min, respectively. From the results shown in Figure 4 as polarization curves, it was noticed that the cell performance improved as the torque increased from 2 N.m to 3 N.m, the reason being that higher bolt torque lowers the electrical contact resistance between the GDL and its neighbouring gas distributor plate and reduce the ohmic overpotential. In addition, higher compression force

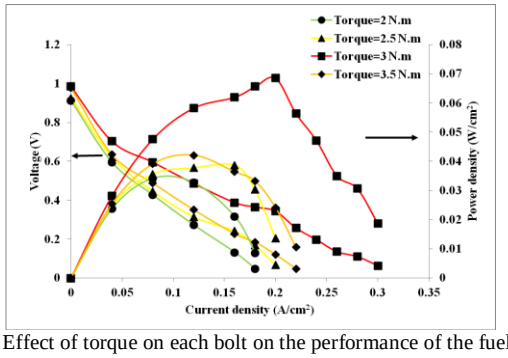

Fig.4 Effect of torque on each bolt on the performance of the fuel cell

changes the hold up of water at the electrodes and the electrochemical reaction area, reducing the concentration overpotential too. This increases the limiting current density from 0.18 A/cm^2 for a torque of 2 N.m to 0.3 A/cm^2 for 3 N.m, as observed in Figure 4. But, increasing the clamping bolt torque beyond 3 N.m, causes the thickness loss of the GDL and hence decrease its porosity and permeability, resulting in lower reactant concentration at the reaction sites [13]. This could be the reason for the decrease in the performance of the fuel cell beyond 3 N.m reducing the current density to 0.22 A/cm^2 at 3.5 N.m. Similarly, the maximum power density also increases from 0.0326 W/cm^2 for a torque of 2 N.m to 0.0685 W/cm^2 for 3 N.m, also shifts towards right along higher current density. This indicates the rate of water removal is enhanced at the cathode membrane interface, delaying the flooding of water at the catalyst sites. Even though this observation was consistent with the results presented by Lee *et al.* [1], the maximum current density obtained was different since they carried out experiments with a PRIMEA series 5000 MEA coated with catalyst 0.3 mg/cm^2 Pt loading with membrane area of 10 cm^2. Anode and cathode humidification temperatures were 85°C and 75°C, respectively and the fuel cell temperature was kept at 80°C.

3.2. Effect of operating parameters on the performance of the fuel cell at the optimum bolt torque

3.2.1 Effect of Anode humidification temperatures (AHT)

To study the effect of AHT on the cell performance at the optimized torque of 3 N.m, two sets of experiments, at TFC of 40°C and 80°C by varying AHT from 40 to 80°C, were conducted [Figures 5(a) and (b)]. For both the sets of experiments, CHT was kept at 50°C and the hydrogen and oxygen mass flow rates were regulated at 100 ml/min and 200 ml/min, respectively. From the polarization curves it was observed that the fuel cell performance reduced as AHT increased, this reduction being less at small and medium current flow indicating that the activation and ohmic losses does not vary significantly with increase in AHT. But, at higher current flow, this effect was found to be significant and observed a decrease in limiting current density with increase in AHT. This is because, with the increase in AHT, the net water content at the anode side of the membrane increases reducing the back diffusion of water from the cathode to the anode. In addition, water transport through the electro-osmotic drag process also increase at increased AHT, accumulating more water at the cathode side. This combined effect increased the flooding at the cathode reducing the limiting current density and thereby reducing the performance of the fuel cell. At lower AHT, the limiting current density increased since the hydrogen concentration at the anode side increase decreasing the water concentration at the anode side. Therefore, the water concentration gradient between cathode and anode increase which not only reduce the cathode flooding, but also improve the cell performance [25]. Yan *et al.* [26] experimentally too observed that, the net electro-osmotic drag coefficient increased with AHT. However, AHT above 60°C, the polarization curves almost coincide which indicate that the cell performance does not vary significantly.

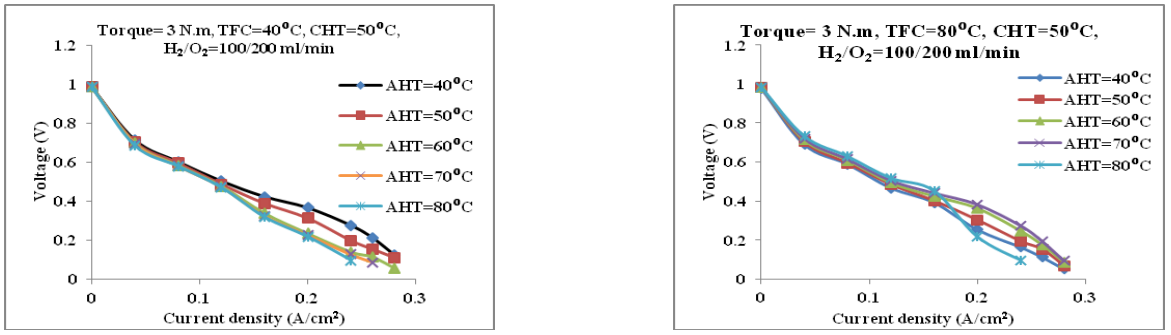

Fig.5. Polarization curves for different AHTs; (a) TFC=40°C; (b) TFC=80°C;

When the fuel cell was operated at higher temperature (80°C), its performance improved with increase in AHT from 40°C to 70°C and reduced at 80°C as shown in Figure 5(b). Higher TFC lead to increased rate of evaporation resulting in membrane dehydration at the anode side at low AHT. At higher current denisties, the performance improved further, since the water diffusion coefficient increased with the fuel cell temperature, improving the water transport by back diffusion reducing the flooding at the cathode. Wang and Liu [27] conducted experiments by increasing the AHT from 40°C to 90°C with TFC maintained at 70°C and reported that the performance increased

with AHT at all levels. From Figure 5(b) at AHT 80°C, below 0.5 V the performance of fuel cell suddenly decreased. This might be because of increase in net electro-osmotic drag causing more water to accumulate at the cathode side reducing the cell performance.

3.2.2 Effect of cathode humidification temperatures (CHT)

To study the effect of CHT on the cell performance at the optimized bolt torque of 3 N.m, CHT was varied from 40°C to 80°C at a TFC of 40°C, and AHT of 50°C and the hydrogen and oxygen mass flow rates at 100 ml/min and 200 ml/min, respectively. The polarization curves presented in Figure 6 indicate that the fuel cell performance decrease as CHT increase from 40 to 80°C. This is because since more water is carried through the inlet oxygen to the cathode membrane interface, the capacity of the gas stream to remove water through evaporation reduces causing flooding at the cathode membrane interface even at low current flow.

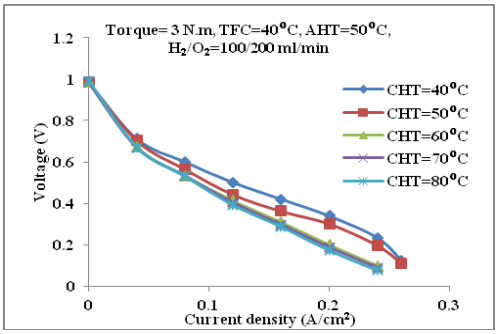

Fig.6. Polarization curves for different CHTs

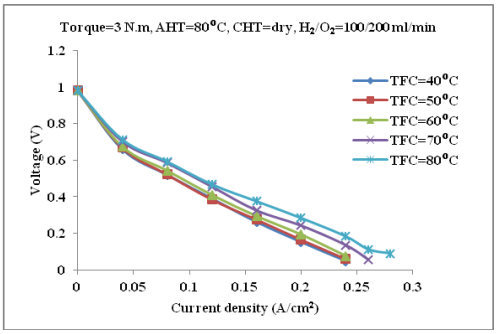

Fig.7. Polarization curves for different TFCs

Rao *et al.* [28] studied that lower CHT was favourable to get the maximum current draw without flooding at the cathode membrane interface. Wang *et al.* [29] also observed experimentally that the limiting current density decreased with increase in CHT from 40°C to 80°C, due to the decreased effective porosity of the GDL, reducing reactant concentration at the cathode catalyst layer. Natarajan and Nguyen [30] have also observed that the cell performance decreases with increase in CHT.

3.2.3 Effect of fuel cell temperature (TFC)

To study the effect of TFC on the cell performance at the optimized bolt torque of 3 N.m, TFC was varied from 40°C to 80°C and the hydrogen and oxygen mass flow rates regulated at 100 ml/min and 200 ml/min, respectively. The anode and cathode reactant temperatures were kept at 80°C and dry, respectively, since there is a possibility of the membrane getting dehydrated at the anode side at higher temperatures. The performance and the limiting current density of the fuel cell increase with TFC as seen in the polarization curves (Figure 7). The exchange current density of the oxygen reduction reaction increases rapidly with increase in TFC reducing the activation losses. High cell temperature improves the proton conductivity of the membrane reducing the ohmic losses and improves the back diffusion of water. High cell temperature also increase the rate of evaporation reducing water content at the cathode side, reducing the concentration loses. The decrease in all the three loses improves the cell performance. This result is consistent with the results published by researchers [27, 28, 29, 31, 32].

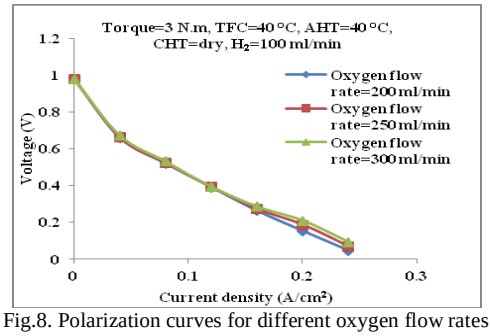

Fig.8. Polarization curves for different oxygen flow rates

3.2.4 Effect of cathode reactant flow rate

To study the effect of cathode reactant flow rate on the cell performance at the optimized bolt torque of 3 N.m, three oxygen flow rates of 200, 250 and 300 ml/min were considered. AHT of 40°C, CHT as dry, TFC of 40°C and the hydrogen mass flow rate was fixed at 100 ml/min. As seen from the polarization curves presented in Figure 8, the effect of oxygen flow rate was found to be almost negligible in the activation and ohmic overpotential region and significant in the concentration overpotential region. This effect could be explained as, by increasing the oxygen flow rate, larger amount of water could be removed from the cathode and also increase back diffusion of water from cathode to anode which results in the increase in cell performance at higher current density region. The water removal rate increase with increase in cathode reactant flow rate improving the cell performance [18, 24].

4. Conclusions

In this work, experiments were carried out on a single transparent PEM fuel cell made up of titanium gas distributor plates with serpentine flow design to discuss the influence of the optimized clamping pressure due to torque applied on each bolt and operating parameters such as AHT, CHT, TFC and cathode reactant flow rates on the performance of the PEM fuel cell.

The following conclusions could be drawn based on the results:

- As the torque applied on each bolt increase, the electrical contact resistance between GDL and gas distributor plate would decrease improving the cell performance. However, the porosity and permeability of the GDL decrease with further increase in torque reducing the cell performance. This combined effect shows that, the performance of the fuel cell increase first to a maximum and then decrease with further increase in the bolt torque.
- The performance of the fuel cell decrease with increasing AHT when the cell operates at low temperature (40°C) and increase with increasing AHT when the cell operates at higher temperature (80°C). This indicates that the anode stream must be humidified to improve the performance of the fuel cell.
- The performance of the fuel cell decrease with increasing CHT and this effect was less significant above 60 °C.
- The performance of the fuel cell increase with TFC. The limiting current density of the fuel cell also increased from 240 mA/cm^2 to 280 mA/cm^2 when the cell temperature increases from 40°C to 80°C.
- The effect of cathode reactant flow rate was almost negligible in the activation and ohmic overpotential region, but was significant in the concentration overpotential region.

Acknowledgements

The authors would like to thank *Ingsman Energy and Fuel cell Research Organization Private Limited* (IEFRO), Chennai, India for the facilities and also thank Dr. Mani for the technical support during this research work.

References

[1] Lee W, Ho CH, Zee JWV, Murthy M. The effect of compression and gas diffusion layers on the performance of a PEM fuel cell. Journal of Power Sources 1999; 84:45-51.

[2] Ge J, Higier A, Liu H. Effect of gas diffusion layer compression on PEM fuel cell performance. Journal of Power Sources 2006; 159:922-27.

[3] Zhou P, Wu CW, Ma GJ. Influence of clamping force on the performance of PEMFCs. Journal of Power Sources 2006; 163:874-81.

[4] Chang WR, Hwang JJ, Weng FB, Chan SH. Effect of clamping pressure on the performance of a PEM fuel cell. Journal of Power Sources 2007; 166:149-54.

[5] Ous T, Arcoumanis C. Effect of compressive force on the performance of a proton exchange membrane fuel cell. Journal of Mechanical Engineering Science 2007; 221:1-8.

[6] Wang X, Song Y, Zhang B. Experimental study on clamping pressure distribution in PEM fuel cells. Journal of Power Sources 2008; 179:305-09.

[7] Lin JH, Chen WH, Yen JS, Ko TH. Effect of gas diffusion layer compression on the performance in a proton exchange membrane fuel cell. Fuel 2008; 87:2420-24.

[8] Wen CY, Lin YS, Lu CH. Experimental study of clamping effects on the performances of a single proton exchange membrane fuel cell and a 10-cell stack. Journal of Power Sources 2009; 192:475-85.

[9] Zhou Y, Lin G, Shih AJ, Hu SJ. Multiphysics Modeling of Assembly Pressure Effects on Proton Exchange Membrane Fuel Cell Performance. Journal of Fuel Cell Science and Technology 2009; 041005:1-7.
[10] Yim SD, Kim BJ, Sohn YJ, Yoon YG, Park GG, Lee WY. The influence of stack clamping pressure on the performance of PEM fuel cell stack. Current Applied Physics 2010; 10:S59-61.
[11] Xing XQ, Lum KW, Poh HJ, Wu YL. Optimization of assembly clamping pressure on performance of proton-exchange membrane fuel cells. Journal of Power Sources 2010; 195:62-68.
[12] Shi Z, Wang X, Guessous L. Effect of Compression on the Water Management of a Proton Exchange Membrane Fuel Cell With Different Gas Diffusion Layers. Journal of fuel cell science and technology 2010; 021012:1-7.
[13] Diedrichs A, Rastedt M, Pinar FJ, Wagner P. Effect of compression on the performance of a HT-PEM fuel cell. Journal of Applied Electrochemistry 2013; 43:1079-99.
[14] Tuber K, Pocza D, Hebling C. Visualization of water buildup in the cathode of a transparent PEM fuel cell. Journal of Power Sources 2003; 124:403-14.
[15] Hakenjos A, Muenter H, Wittstadt U, Hebling C. A PEM fuel cell for combined measurement of current and temperature distribution, and flow field flooding. Journal of Power Sources 2004; 131:213-16.
[16] Yang XG, Zhang FY, Lubawy AL, Wang CY. Visualization of Liquid Water Transport in a PEFC. Electrochemical and Solid-State Letters 2004; 7: A408-11.
[17] Sugiura K, Nakata M, Yodo T, Nishiguchi Y, Yamauchi M, Itoh Y. Evaluation of a cathode gas channel with a water absorption layer/waste channel in a PEFC by using visualization technique. Journal of Power Sources 2005; 145:526-33.
[18] Liu X, Guo H, Ma C. Water flooding and two-phase flow in cathode channels of proton exchange membrane fuel cells. Journal of Power Sources 2006; 156:267-80.
[19] Zhang FY, Yang XG, Wang CY. Liquid Water Removal from a Polymer Electrolyte Fuel Cell. Journal of the Electrochemical Society 2006; 153:A225-32.
[20] Weng FB, Su A, Hsu CY, Lee CY. Study of water flooding behaviour in cathode channel of a transparent proton-exchange membrane fuel cell. Journal of Power Sources 2006; 157:674-80.
[21] Su A, Weng FB, Hsu CY, Chen YM. Studies on flooding in PEM fuel cell cathode channels. International Journal of Hydrogen Energy 2006; 31:1031-39.
[22] Liu X, Guo H, Ye F, Ma CF. Water flooding and pressure drop characteristics in flow channels of proton exchange membrane fuel cells. Electrochimica Acta 2007; 52:3607-14.
[23] Spernjak D, Prasad AK, Advani SG. Experimental investigation of liquid water formation and transport in a transparent single-serpentine PEM fuel cell. Journal of Power Sources 2007; 170:334-44.
[24] Ous T, Arcoumanis C. Visualisation of water accumulation in the flow channels of PEMFC under various operating conditions. Journal of Power Sources 2009; 187:182-89.
[25] Lee D, Bae J. Visualization of flooding in a single cell and stacks by using a newly-designed transparent PEMFC. International Journal of Hydrogen Energy 2012; 37:422-35.
[26] Yan Q, Toghiani H, Wu J. Investigation of water transport through membrane in a PEM fuel cell by water balance experiments. Journal of Power Sources 2006; 158:316-25.
[27] Wang L, Liu H. Performance studies of PEM fuel cells with interdigitated flow fields. Journal of Power Sources 2004; 134:185-96.
[28] Rao SSL, Shaija A, Jayaraj S. Optimization of operating parameters to maximize the current density without flooding at the cathode membrane interface of a PEM fuel cell using Taguchi method and genetic algorithm. International Journal of Energy and Environment 2014; 5:335-52.
[29] Wang L, Husar A, Zhou T, Liu H. A parametric study of PEM fuel cell performances. International Journal of Hydrogen Energy 2003; 28:1263-70.
[30] Natarajan D, Nguyen TV. Three- dimensional effects of liquid water flooding in the cathode of a PEM fuel cell. Journal of Power Sources 2003; 115:66-80.
[31] Amirinejad M, Rowshanzamir S, Eikani MH. Effects of operating parameters on performance of a proton exchange membrane fuel cell. Journal of Power Sources 2006; 161:872-75.
[32] Mulyazmi, Daud WRW, Majlan EH, Rosli MI. Water balance for the design of a PEM fuel system. International Journal of Hydrogen Energy 2013; 38:9409-20.